SEMARAK ILMU PUBLISHING

Journal of Advanced Research in Applied Mechanics

Journal homepage:
https://semarakilmu.com.my/journals/index.php/appl_mech/index
ISSN: 2289-7895

Microcrystalline Cellulose Based Adsorbent Derived from Watermelon Rind for Dye Removal

Julie Ho Min Hui[1], Yeu Yee Lee[1,*], Charlie Sia Chin Voon[1], Soon Kok Heng[1]

[1] Faculty of Engineering, Computing and Science, Swinburne University of Technology (Sarawak Campus), 93350 Kuching, Sarawak, Malaysia

ARTICLE INFO

Article history:
Received 3 May 2024
Received in revised form 28 June 2024
Accepted 11 July 2024
Available online 30 July 2024

Keywords:
Microcrystalline cellulose; Bio-sorbent; Dye removal; Methylene blue adsorption

ABSTRACT

This study investigated the potential of watermelon rind derived microcrystalline cellulose (MCC) for the removal of methylene blue dye from aqueous solutions. The objectives were to evaluate the adsorption capabilities of watermelon rind derived MCC and assess the effect of process variables on its adsorption capacity. FTIR analysis was conducted to compare the absorption patterns of untreated watermelon rind and MCC. The absence of peaks at 1720, 1584, and 1242 cm^{-1} in the MCC spectra confirmed the successful removal of lignin and hemicellulose from the sample. Thermogravimetric analysis showed that MCC exhibited an earlier onset of degradation compared to watermelon rind and reached its peak degradation rate at 215°C, as indicated in the DTG curve. The scanning electron microscopy analysis revealed that the MCC exhibited a rod-like shape with a diameter of less than 74 µm and a length of less than 737 µm. With an intermittent breakdown of the fibrillar structure into individualised fibrils, this unique morphology provides a larger surface area for adsorption, thus increasing the potential of MCC as a bio-adsorbent. The adsorption behaviour of MCC in aqueous solution was then investigated, specifically focusing on the impact of contact time and initial dye concentration on its adsorption capacity. The results demonstrated that the optimum dye removal efficiency of 86.32% was achieved when the methylene blue dye concentration was 1.5 mg/L. Furthermore, the dye removal efficiency rapidly increased from 67.34% to 80.73% as the contact time increased from 20 minutes to 60 minutes, after which the rate of increase slowed down significantly. These findings highlight the importance of optimising these variables to maximise the adsorption potential of MCC for efficiently removing contaminants. These findings contribute to the development of sustainable and cost-effective methods for particle removal in water treatment applications.

1. Introduction

The 21st century presents significant challenges for the global food and agricultural sector, with approximately 33% of food produced for human consumption being wasted worldwide and fruits being the highest contributors to this statistic [1,2]. A substantial amount of waste materials, including peels, seeds, and unused flesh, is generated throughout the fruit processing chain.

* *Corresponding author.*
E-mail address: yyeu@swinburne.edu.my

https://doi.org/10.37934/aram.122.1.130146

Regrettably, these waste products are often discarded into the environment despite containing valuable compounds with significant economic potential. Consequently, the disposal of fruit waste results in substantial wastage and contributes to environmental issues such as soil erosion and water pollution.

The utilisation of fruit waste for dye removal in wastewater treatment plants can significantly benefit the textile industry. With global annual consumption of more than 107 kg, dyes discharged into the environment have become a major concern, particularly in developing countries [3]. Methylene blue (MB) is a triphenyl cationic azo dye, also known as Hexamethyl pararosaniline chloride, with the molecular formula of $C_{16}H_{18}N_3SCl$, widely used in pharmaceutical, food, and textile industries for dyeing cotton, wood, and silk [4]. It poses health risks, including eye burns, respiratory difficulties, and mental confusion upon exposure [5]. Consequently, it is crucial to employ various physical, chemical, and biological treatment methods to address this issue [6-8]. Among these approaches, adsorption is recognized as one of the most effective techniques for dye removal, given its economic viability and environmental compatibility [9].

Cellulose, a widely available carbon polymer found in various plant, animal, and bacterial sources, constitutes a significant portion of food waste [10]. It possesses long chains of linear homopolysaccharide β-d-glucopyranose units linked together by β-1-4-linkages, in which inter and intramolecular hydrogen bonds help cellulose to have a crystalline structure and enable the fibril aggregation [11,12]. Cellulose has four polymorphs, namely cellulose I, II, III, and IV [13]. Cellulose I is the naturally occurring cellulose in parallel strands without intersheet hydrogen bonding [14]. Cellulose II is thermodynamically more stable with high surface area, surface accessibility, and antiparallel strains with intersheet hydrogen bonding [15]. The main difference between cellulose I and II properties is due to the bonding between the cellulose chains or crystal structure changes. However, this remains a question of intense debate [16]. Cellulose III is amorphous and can be formed from cellulose I and II by the treatment with amines [17]. Cellulose IV can be obtained by modifying cellulose III with glycerol at very high temperatures [18]. The amorphous nature of cellulose renders it susceptible to acid hydrolysis, producing microcrystalline cellulose (MCC) by disrupting the amorphous regions [19].

MCC derived from crystalline units has garnered considerable attention as an adsorbent among researchers in recent decades [20,21]. This is primarily due to its advantageous features, including a high surface area, abundance, low cost, and biodegradability [22]. The formation of MCC through acid hydrolysis is commonly achieved using sulfuric acid, as it generates MCC with a surface charge and stable colloidal dispersion [23]. The hydrolysis process with sulfuric acid introduces sulfate ester groups, resulting in negative charges on the surface of MCC. Consequently, these negative charges facilitate electrostatic repulsion in aqueous solutions, promoting uniform dispersion of microcrystals [24]. Moreover, the presence of negative charges on the MCC surface makes it a promising candidate for use as an adsorbent, as it exhibits a high adsorption capacity for the removal of positively charged dyes [25].

The adsorbent derived from MCC extracted from waste banana pseudo-stem achieved a notable adsorption capacity of 40.16 mg/g at room temperature to remove MB in aqueous solution [23]. In comparison, MCC extracted from oil palm fronds demonstrated promising potential as an MB adsorbent, achieving 51.81 mg/g [26]. Meanwhile, MCC extracted from cotton fibre showed an even higher maximum adsorption capacity for MB, reaching 115.2 mg/g [27]. These findings underscore the significant potential of MCC derived from biomass waste in effectively removing MB dye from aqueous solutions.

The increased demand for wood and wood-based products in the commercial production of MCC has raised concerns regarding deforestation and sustainability [28]. As a result, the focus has shifted

towards exploring alternative and underutilised renewable materials for MCC extraction [29]. Fruit waste presents a viable option as it can economically replace solid wood as a precursor for MCC production [30]. Based on the study conducted by Ahmad *et al.*, [31] MCC extracted from rice husk can achieve up to 83.26% yield. Additionally, in the study by Abdullah *et al.*, [32] and Debnath *et al.*, [33], various biomasses were investigated for microcrystalline cellulose (MCC) extraction, revealing noteworthy yields. Water hyacinth demonstrates an MCC yield of 73.76%, sweet sorghum reaches 81.8%, kans grass achieves 83%, soybean hulls demonstrate a yield of 83.8%, waste cotton fabrics show 83.4%, sacred Bali bamboo can achieve up to 84.9%, tea waste demonstrates 86.7%, Sengon wood exhibits a yield of 89.46%, and kapok fibre boasts an impressive 91.21% yield.

In this study, watermelon rind was selected as the cellulose source. Watermelon (*Citrullus lanatus*), belonging to the *Cucurbitaceae* family, is a widely cultivated flowering plant with over 1000 varieties [34]. While the fruit is edible and consumed by humans, the outer skin or rind of the watermelon is often discarded as waste. The watermelon rind accounts for approximately 30% of the total fruit mass and lacks economic value, creating a significant environmental disposal challenge [35]. Therefore, exploring the potential of watermelon rind as a source of cellulose for MCC extraction not only addresses the waste management issue but also offers a sustainable and environmentally friendly alternative to traditional wood-based sources.

Considering the widespread abundance of watermelon rind as a waste product, this study aims to transform this underutilized material into a more valuable resource in the form of MCC. The primary objectives of this study are twofold: first, to characterize the MCC extracted from watermelon rind, and second, to investigate the efficiency of MCC in removing dyes from solution by examining the influence of contact time and dye concentration. By accomplishing these objectives, this research seeks to contribute to understanding MCC properties derived from watermelon rind and explore its potential application as an effective dye adsorbent.

2. Materials and Methods

2.1 Materials

Watermelon rinds were obtained from a local market in Kuching, Malaysia, and served as the raw material for the extraction of MCC. All chemicals, including sodium hydroxide pellets, 30% hydrogen peroxide (H_2O_2), 95% sulphuric acid (H_2SO_4), 99.5% anhydrous tert-butanol, and MB, were of analytical grade acquired from Sigma-Aldrich Chemicals. Distilled water was used to dilute all solutions used in this study as necessary.

2.2 Pre-Treatment of Watermelon Rind

The raw watermelon rind was initially sliced into small pieces and dried in an oven at 40°C for 24 hours. Following the drying process, the watermelon rind was further fragmented into smaller pieces, with lengths ranging from 0.3 to 0.7 cm and widths ranging from 0.1 to 0.2 cm.

To initiate the alkaline treatment, 2 g of dried watermelon rind was combined with 100 mL of 9% NaOH solution in a 250 mL beaker. The mixture was stirred using a magnetic stirrer at a constant speed for 60 minutes while maintaining a temperature range of 70 to 80°C. The purpose of this step was to dissolve and remove non-cellulosic components, specifically lignin and hemicellulose, which are soluble in alkali [36].

Following the treatment, the watermelon rind was thoroughly washed with distilled water until a neutral pH of 7 was achieved. This step ensured the removal of residual alkali from the treated material. Subsequently, the recovered residue was subjected to drying at 50°C for 24 hours—the

drying process aimed to obtain a dry and stable sample for subsequent analysis and further processing.

The delignification step was conducted following the procedure by Wijaya *et al.*, [37]. This step removes lignin from the inter-fibril spaces, exposing the amorphous and crystalline cellulose regions for subsequent acid hydrolysis. The treatment involved immersing 0.3 g of alkaline-treated fibres in a solution comprising 10 mL of 4% NaOH and 10 mL of 30% H_2O_2. The mixture was continuously stirred using a magnetic stirrer for 60 minutes at 50 to 60°C.

After completion of the delignification process, the bleached fibres were separated from the solution by filtration using a filter funnel. The filtered fibres were then thoroughly washed with distilled water until the washing solution reached a neutral pH. This ensured the removal of residual chemicals from the bleached fibres. Subsequently, the bleached fibres were dried at 50°C for 24 hours to obtain a dry and stable sample for further analysis and experimentation.

2.3 Sulphuric Acid Hydrolysis

The extraction of MCC was carried out through acid hydrolysis of the previously bleached fibres, following an established method [9]. Initially, 0.3 g of the bleached fibres was added to 3 mL of preheated 58% sulphuric acid solution at 55°C. The mixture was then placed in a water bath and stirred continuously at a fixed speed for 60 minutes.

Following the acid hydrolysis, the mixture was diluted with 47 mL of distilled water, and the resulting dispersion was subjected to centrifugation at 6000 rpm for 5 minutes. The precipitate was collected and transferred into a dialysis tube to remove non-reactive sulphate groups, salts, and soluble sugars. The dialysis tube containing the precipitate was placed in a beaker filled with distilled water, and the water in the beaker was changed daily until the distilled water reached a neutral pH.

2.4 Addition of Surfactant Prior to Oven drying

The cellulose suspension obtained from the dialysis process was adjusted to a concentration of 0.1 wt% by adding distilled water. Before oven drying, 9 mL of the suspension was mixed with 1 mL of tert-butanol (t-BuOH), as previously conducted by Hanif *et al.*, [38]. This is because drying in the oven often results in interfibrillar aggregation, making it difficult for subsequent aqueous re-dispersion. Using t-BuOH helps minimise interfibrillar shrinkage because t-BuOH has lower surface tension than water. The remaining t-BuOH/water mixture will also reduce interfibrillar adhesion and contact. The mixture was then dried in an oven at 100°C for 24 hours. The dried MCC was collected once the drying process was finished.

The yield of MCC was determined using Eq. (1), where the weight of MCC obtained was divided by the initial weight of the bleached fibres used in the extraction process.

$$\text{Yield of MCC (\%)} = \frac{\text{Weight of MCC dry sample}}{\text{Initial weight of cellulose}} \times 100\% \quad (1)$$

2.5 Characterisation

2.5.1 Scanning electron microscopy

Scanning electron microscopy (SEM) was conducted to investigate the morphology of both untreated watermelon rind and MCC. The SEM analysis was performed using a scanning electron microscope (Joel JSM-6000) operated at an acceleration voltage of 10-20 kV. Before the SEM

analyses, the samples were coated with a thin layer of gold using a coating system to ensure adequate conductivity and enhance the imaging quality. This gold coating process is essential for achieving accurate and detailed SEM images of the samples.

2.5.2 Fourier transform infrared spectroscopy

Fourier Transform Infrared (FTIR) spectroscopy (Thermo Scientific Nicolet™ Summit Spectrometer) was employed to analyse the functional groups in both watermelon rind and MCC. To prepare the samples for FTIR analysis, they were mixed with potassium bromide (KBr) and compressed into pellets. This palletisation process facilitated the uniform distribution of the sample and ensured consistent results during the FTIR analysis. The FTIR analysis was conducted within a wavelength range of 4000 to 450 cm^{-1}, enabling the identification and characterisation of the various functional groups in the samples.

2.5.3 Thermogravimetric analysis

Thermogravimetric analysis (TGA) was performed using Perkin Elmer STA 8000 to assess the thermal stability of both untreated watermelon rind and MCC samples, allowing the generation of thermogravimetric (TG) and derivative thermogravimetric (DTG) curves. The analysis was conducted under an inert atmosphere with a continuous flow of nitrogen gas at a 20 mL/min rate.

Approximately 3-4 mg of the material was carefully placed into an aluminium crucible for each sample. The TGA measurement involved heating the samples from 40 to 600°C at a controlled heating and cooling rate of 10°C/min, as described by Chieng *et al.*, [39].

By monitoring the weight loss of the samples as a function of temperature, the TG curves provided information on the thermal stability and decomposition behaviour of the materials. The DTG curves, derived from the TG data, revealed the weight loss rate as a temperature function.

2.6 Performance Test of MCC as Adsorbent

2.6.1 Dye concentration and absorbance

The adsorption of MB onto the MCC adsorbent was investigated in this study. To initiate the adsorption process, stock solutions of MB and MCC were prepared. Specifically, 10 mL of the MB solution and 0.02 g of MCC were mixed in a 50 mL beaker. The mixture was agitated using a magnetic stirrer at 250 rpm for 60 minutes.

After the agitation period, the stirrer bar was removed, and the mixture was centrifugated at 5000 rpm for 5 minutes. The supernatant was collected, and the initial and final absorbance of the MB solution was measured using a UV-Vis spectrophotometer at a wavelength of 682 nm.

A calibration curve was constructed to determine the concentration of MB in the solution by plotting the absorbance values against the known concentrations of MB at 682 nm. This calibration curve allowed for the conversion of the adsorption values of free dye molecules to their corresponding concentrations.

The removal efficiency of MB and the amount adsorbed onto the MCC adsorbent were calculated using Eq. (2) and Eq. (3), respectively [8], as follows:

$$R_{MB} = \frac{C_o - C_e}{C_o} \times 100\% \quad (2)$$

$$q_e = \frac{C_o - C_e}{m} V \quad (3)$$

where R_{MB} is the dye removal percentage, q_e is the amount of dye adsorbed for 1 g of adsorbent (mg/g), C_o is the initial dye concentration (mg/L), C_e is the equilibrium concentration of free dye molecules in the solution (mg/L), m is the mass of adsorbent (g) and V is the volume of solution (L).

2.6.2 Batch adsorption test
2.6.2.1 Effect of contact time

The effect of contact time on the adsorption process was investigated by varying the duration from 20 to 60 minutes while maintaining a constant adsorbent dosage of 0.02 g. This approach facilitated an examination of the dynamic evolution of the adsorption of the target species, such as MB, onto the MCC adsorbent. By observing the adsorption kinetics at different contact times, valuable insights can be gained into the rate and efficiency of the adsorption process.

2.6.2.2 Effect of initial dye concentration

The effect of initial concentration on the adsorption process was assessed by adjusting the dye concentration within the 0.5 to 3.0 mg/L range. To ensure a consistent contact time, the best contact time obtained from the previous investigation (60 minutes) was maintained throughout this experiment. By examining the adsorption performance at different initial concentrations, insights into the capacity and efficiency of the MCC adsorbent can be obtained. This analysis helps to determine the optimal conditions for achieving effective dye removal and provides valuable information on the adsorption behaviour of the MCC adsorbent under varying initial concentration conditions.

3. Results and Discussions

3.1 Yield of MCC

According to a study by Ibrahim *et al.*, [40], the yield of cellulose obtained from watermelon rind was reported to be 20%. Given this moderate yield, the utilisation of watermelon rind for the preparation of MCC was considered. In our study, the yield of MCC was determined after subjecting the cellulose extracted from watermelon rind to acid hydrolysis for 60 minutes. The yield of MCC was calculated using Eq. (1) and was found to be 13.97%.

3.2 Morphology

Scanning electron microscopy (SEM) or SEM analysis was used to examine the surface morphology of watermelon rind (WR) fibres, and MCC obtained through chemical purification and acid hydrolysis. Figure 1 displays the SEM image of WR, while Figure 2 shows the SEM image of MCC derived from WR.

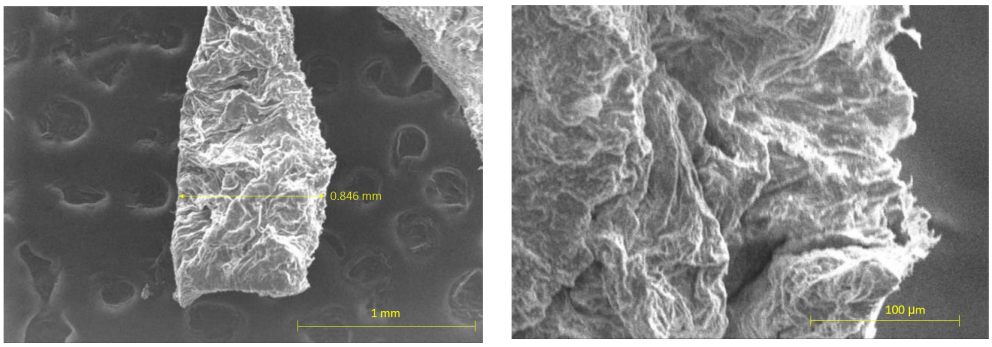

(a) (b)

Fig. 1. SEM image of WR under two magnifications (a) 120x and (b) 1000x

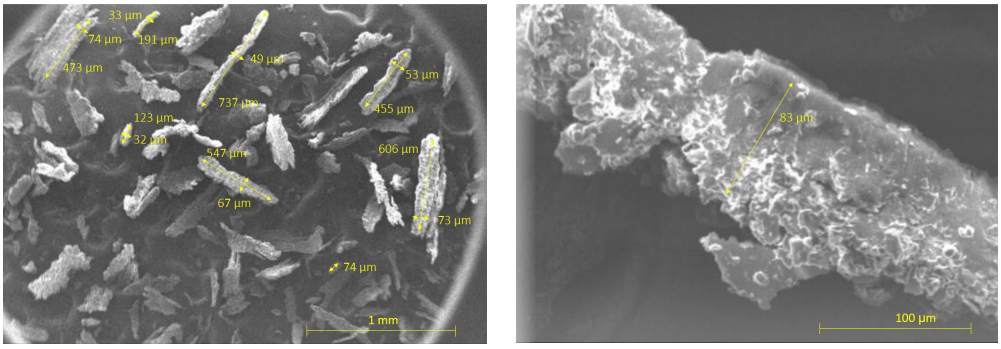

(a) (b)

Fig. 2. SEM image of MCC derived from WR under two magnifications (a) 100x and (b) 1000x

The SEM analysis revealed that the surface of WR exhibited an irregular and non-smooth appearance, indicating the presence of impurities and structural imperfections. In contrast, the surface of MCC appeared smoother and exhibited a wrinkled structure [41]. This observation suggests the successful removal of hemicelluloses, lignin, pectin, and other impurities during the purification and acid hydrolysis.

Furthermore, the SEM micrographs of MCC displayed in Figure 2 provided evidence of a reduction in the size of the fibrillar structure. This reduction can be attributed to the removal of amorphous parts of cellulose and the intermittent breakdown of the fibrillar structure into individualized fibrils. These findings confirm the efficiency of adding tert-butanol to MCC before the oven drying process, as it successfully prevented MCC aggregation during drying.

The rod-like structure observed in Figure 2 is consistent with previous reports on MCC derived from oil palm empty fruit bunch [42]. This similarity in structure supports the validity and consistency of the MCC extraction process and the formation of the desired microcrystalline morphology. The measured dimensions of MCC indicate a diameter of less than 74 µm and a length of less than 737 µm.

3.3 Chemical structure of WR and MCC

The FTIR analysis was conducted to examine the functional groups present in both WR and MCC samples. As a lignocellulosic material, WR primarily consisted of polysaccharides (cellulose and hemicellulose) and an aromatic polymer (lignin), resulting in the presence of various functional groups such as alkanes, esters, aromatics, ketones, and alcohols, along with oxygen-containing functional groups [43].

The FTIR spectra of WR and MCC are illustrated in Figure 3. The peaks observed at 3330 cm^{-1} in both WR and MCC spectra indicated the stretching vibrations of the OH group. The peaks at 2882 cm^{-1} for WR and 2890 cm^{-1} for MCC corresponded to the C-H stretching vibrations. The presence of a peak in the range of 1621 – 1637 cm^{-1} represented the bending absorption of water. Notably, the removal of water from the fibres proved to be a challenging task, even though the FTIR samples underwent a proper drying process. Spectral bands at 1400 – 1419 cm^{-1} and 1366 – 1369 cm^{-1} indicated the CH_2 asymmetric bending motion in cellulose and the bending vibrations of the C-H and C-O groups of the aromatic rings in polysaccharides, respectively. The stretching vibration of the C-O-C pyranose ring yielded a prominent peak at 1021 cm^{-1}, and an increase in cellulose content was accompanied by an increment in peak intensity at 1021 cm^{-1} in both samples. Additionally, the observed increase in the peak at 894 – 897 cm^{-1} in Figure 3 provides further evidence of a characteristic cellulose structure, specifically indicating the presence of β-glycosidic linkages within the glucose ring. Additionally, the observed increase in the peak at 894-897 cm-1 in Figure 3 provides further evidence of a characteristic cellulose structure, specifically indicating the presence of β-glycosidic linkages within the glucose ring [44].

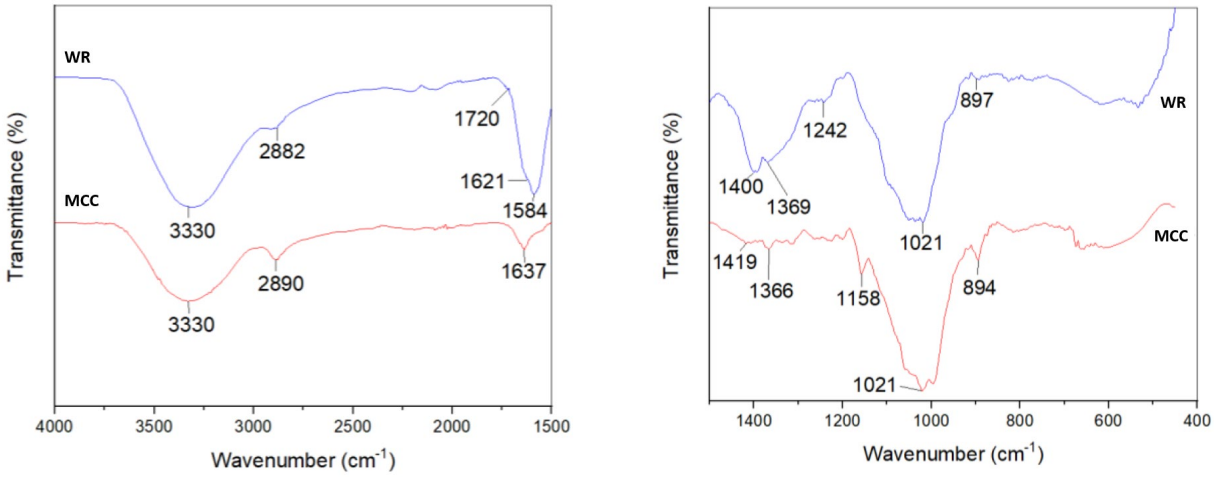

Fig. 3. FTIR spectra of WR (blue) and MCC (red) on the wavelength of (a) 4000 - 1500 cm^{-1} and (b) 1500 – 400 cm^{-1}

A comparison of the IR spectra of WR and MCC revealed changes in the functional groups after acid hydrolysis. The peak observed at 1584 cm^{-1} in the WR spectrum was associated with the characteristics of lignin, representing C=C unsaturated linkages and aromatic rings present in lignin [45]. The primary characteristic peak of hemicellulose was typically identified around 1707 – 1735 cm^{-1} [31, 46]. In the WR sample, a smaller shoulder peak observed at 1720 cm^{-1} corresponds to carboxyl groups, which are associated with the acids and esters of acetic, p-coumaric, ferulic, and uronic acids. These components are primarily found in extractives and hemicellulose, confirming their presence in the watermelon rind sample [47]. Another significant peak associated with hemicellulose was observed at 1242 cm^{-1}, assigned to the acyl-oxygen CO-OR stretching vibration in hemicellulose. The absence of peaks at 1720, 1584, and 1242 cm^{-1} in the MCC spectra indicated the successful removal of hemicellulose and lignin through acid hydrolysis. The sulfate group (SO_2) was also observed in the MCC spectrum at 1158 cm^{-1}, likely resulting from cellulose sulfonation during the sulfuric acid hydrolysis process [48].

3.4 Thermogravimetric Analysis

Thermogravimetric Analysis (TGA) was conducted to evaluate the thermal stability of WR and MCC. The TG and DTG thermograms of WR and MCC are presented in Figures 4(a) and 4(b), respectively.

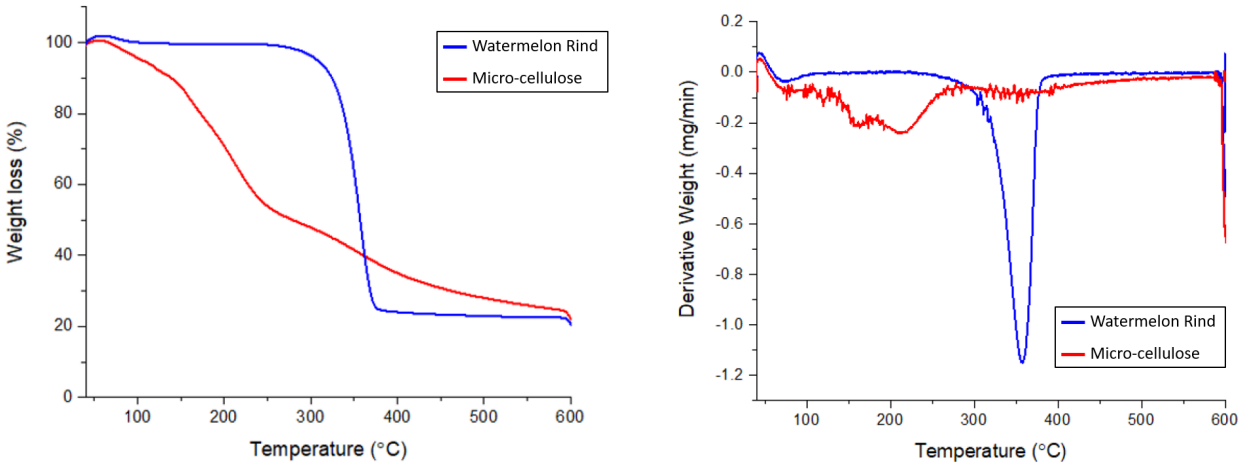

(a) (b)

Fig. 4. (a) TGA and (b) DTG curves for WR and MCC

The TG and DTG thermograms exhibited two distinct weight loss stages for all samples: a low-temperature range below 100°C and a high-temperature range between 100°C and 600°C. The initial weight loss in the low-temperature range (< 10%) can be attributed to water evaporation, as reported by Chieng *et al.,* [39]. Notably, the major weight loss (> 50%) observed in the high-temperature range indicates the primary thermal degradation of the cellulosic samples. During this stage, the degradation of hemicellulose, lignin, and the depolymerization of cellulosic fibres occur. Hemicellulose degradation takes place in the temperature range of 160-250°C, lower than the cellulose, where the degradation occurs between 300-400°C [39,49], while lignin decomposes over a broad range of temperatures 150–900°C [50].

The TGA curve demonstrated that MCC exhibited an earlier onset of degradation compared to WR, as indicated by the DTG curve reaching its peak degradation rate at 215°C. This reduction in thermal stability can be attributed to the presence of sulfate groups on the surface of MCC resulting from sulfuric acid hydrolysis. These sulfate groups are expected to lower the degradation temperature of MCC due to the lower activation energy of decomposition associated with the surface sulfate groups [51, 52]. Beyond 380°C, the residual decomposition products reached a plateau and displayed a slower degradation profile. Interestingly, at the end of the pyrolysis process, the residue content of MCC at 600°C was observed to be higher than that of WR. This behaviour can be attributed to the favoured dehydration effects of the sulfate groups, acting as flame retardants at lower temperatures [53].

3.5 Dye Adsorption Studies

3.5.1 Effect of contact time on methylene blue adsorption

The adsorption profile of MB onto the MCC adsorbent was examined over various contact times, as presented in Figure 5. The findings of this study demonstrate an increase in both the dye removal

percentage and the amount of dye adsorbed as the contact time increased from 20 minutes to 100 minutes, reaching values of 67.34% to 83.12% and 1.01 mg/g to 1.25 mg/g, respectively.

The adsorption of MB by MCC was found to be rapid during the initial stages of contact time, with a higher rate of dye removal observed at the beginning. This can be attributed to the larger surface area and the availability of numerous adsorption sites on the MCC surface, facilitating the rapid adsorption of dye ions [54]. However, after the initial rapid uptake, the adsorption process proceeded slower and eventually reached equilibrium. This phenomenon can be attributed to the deposition of dyes on the accessible adsorption sites of MCC, leading to repulsive interactions between the dye molecules already adsorbed on the MCC surface and the remaining dye molecules, hindering their movement towards the MCC surface [55].

These observations determined an equilibrium time of 60 minutes, representing the point at which the adsorbent, MCC, achieved its maximum adsorption capacity. This suggests that MCC can effectively remove methylene blue from aqueous solutions.

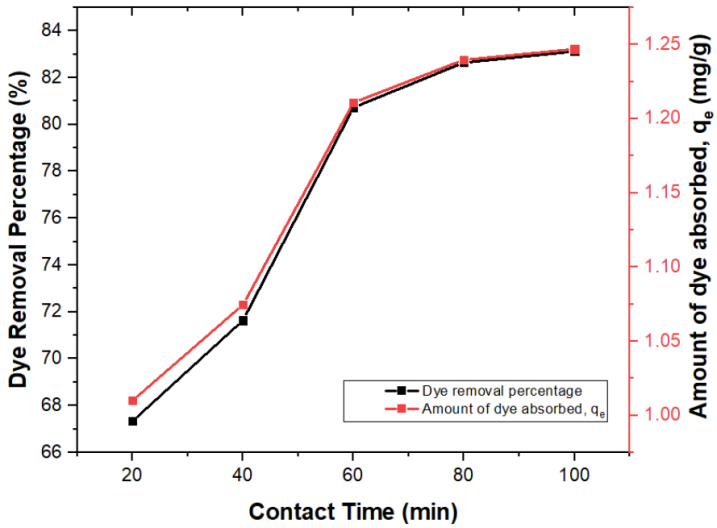

Fig. 5. Effect of contact time on dye removal percentage and amount of dye absorbed

3.5.2 Effect of initial dye concentration on methylene blue adsorption

The effect of initial dye concentration on the percentage of dye removal was investigated, as shown in Figure 6. The findings revealed a distinct trend in the percentage of dye removal concerning the initial dye concentration when a fixed amount of adsorbent was used. Initially, there was an increase in the percentage of dye removal as the initial dye concentration increased. However, beyond a certain point, the percentage of dye removal exhibited a significant decrease. The initial increase in dye removal at lower dye concentrations can be attributed to the low ratio of dye molecules to the number of available adsorption sites on the MCC surface. With fewer dye molecules present, there is a higher chance for them to occupy the available adsorption sites, leading to a higher percentage of dye removal. However, at relatively higher dye concentrations, the ratio of the increase in dye concentration to the increase in the amount of dye absorbed becomes lower. This is due to the limited availability of adsorption sites on the MCC surface compared to the higher number of dye molecules. As a result, the dye removal efficiency decreases as the repulsive forces between the dye molecules hinder their adsorption on the MCC surface [55]. While there is a decrease in the percentage of dye removal as the initial dye concentration increases, it is important to note that the

amount of dye absorbed per unit mass (q_e) increases. This implies that, despite the decrease in percentage, the adsorbent is capable of adsorbing a greater quantity of dye per unit mass at higher initial dye concentrations. Therefore, the MCC adsorbent demonstrates a higher capacity for adsorbing dye molecules at higher initial dye concentrations.

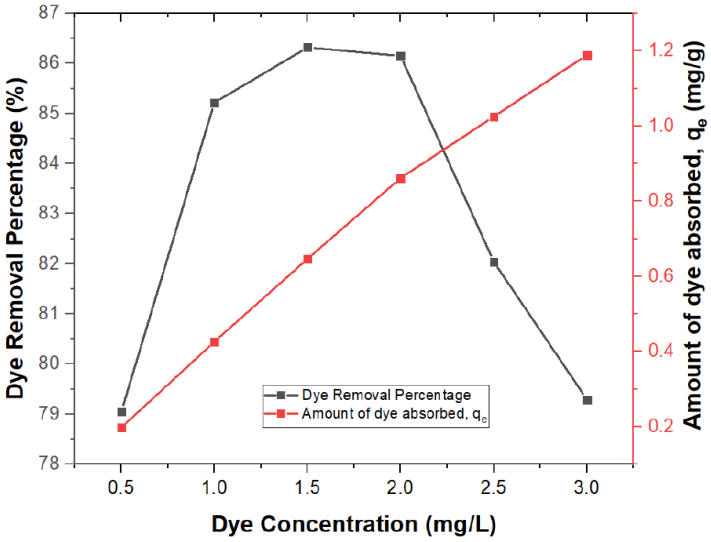

Fig. 6. Effect of initial dye concentration on dye removal percentage and amount of dye absorbed

3.6 Adsorption Isotherms

Adsorption isotherm describes the interaction characteristics between the adsorbate and adsorbents at equilibrium and constant temperatures [56]. It is fundamentally essential in determining the optimal efficiency of the adsorbents. Typically, isotherm data are correlated by employing various isotherm models, and the best-fitting model is selected to analyze adsorption behaviour. Freundlich and Langmuir isotherms are the two commonly used models to predict the adsorption capacity of a specific material. Therefore, the relationship between MB adsorption and dye concentration equilibrium was verified using Langmuir and Freundlich isotherms.

3.6.1 Langmuir isotherm

Langmuir model represents monolayer sorption onto the homogenous adsorbent's surface when no interaction occurs between adsorbed species [57]. The adsorption data are validated by determining the relative parameters of this model using Eq. (4).

$$\frac{1}{q_e} = \frac{1}{K_L q_{max}} \cdot \frac{1}{C_e} + \frac{1}{q_{max}} \tag{4}$$

where q_e is the amount of dye adsorbed at equilibrium (mg/g), and C_e is the equilibrium adsorbate concentration (mg/L). The values of the maximum adsorption capacity of the adsorbent, q_{max} (mg/g), and energy of adsorption, K_L, are estimated from the slope gradient and intercept of the linear plot (Figure 7). To compute adsorption efficiency, the dimensionless constant separation factor, R_L, was obtained using Eq. (5) [58].

$$R_L = \frac{1}{1 + C_i K_L} \tag{5}$$

where C_i is the initial concentration of dye (mg/L), and K_L is the Langmuir isotherm constant related to the sorption energy. The feasibility of adsorption can be evaluated from the values of R_L, which serve as an indicator of the adsorption's favourability. The adsorption is favourable when $0 < R_L < 1$, $R_L > 1$ suggests an unfavourable scenario, $R_L = 1$ indicates linearity, and $R_L = 0$ indicates irreversibility. Table 1 shows that the calculated value of R_L for the initial dye concentration of 1.5 mg/L was 0.8529. The maximum adsorption capacity was 20.54 mg/g. The K_L value of 0.1150, which is slightly greater than 0.1, indicated the affinity of the adsorbent toward dye adsorption. [56].

Table 1
Parameters of Langmuir Isotherm

Langmuir Isotherm	q_{max} (mg/g)	K_L	R_L	R^2
	20.54	0.1150	0.8529	0.9661

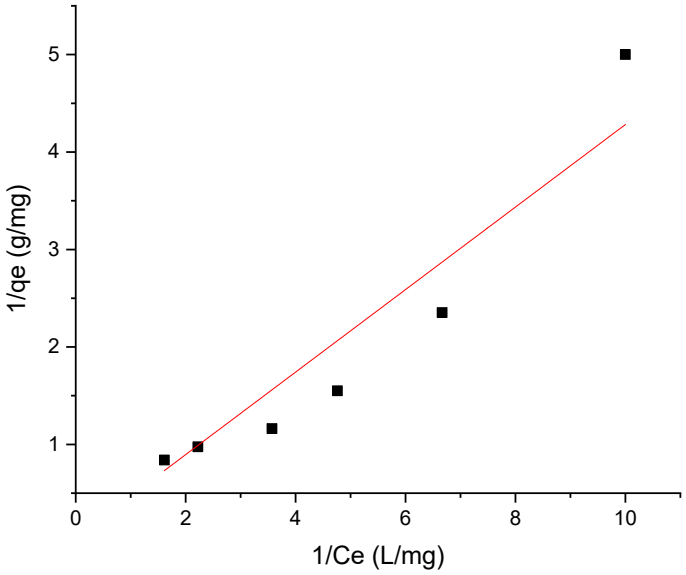

Fig. 7. Langmuir adsorption plot

3.6.2 Freundlich isotherm

Freundlich isotherm is one of the simplest nonlinear sorption models. In contrast to Langmuir, which assumes that ions are adsorbed in a monolayer on the surface and that the greatest adsorption occurs when the surface is fully covered, Freundlich assumes that there exist heterogeneous surfaces with different affinities, allowing for multilayer adsorption [59]. The linearized Freundlich isotherm equation is represented by Eq. (6).

$$\log q_e = \log K_f + \frac{1}{n} \log C_e \tag{6}$$

where q_e is the amount of dye adsorbed per unit mass of adsorbent at equilibrium (mg/g), and C_e is the residual concentration of dyes in the solution at equilibrium (mg/L). Depending on the nature of adsorbate and adsorbent, the Freundlich constants, K_f and n, are relative indicators of the adsorption intensity and the adsorption capacity, respectively [60]. By plotting Eq. (6) as shown in

Figure 8, the value of 1/n can be determined from the slope gradient, and the intercept is equal to log K_f.

Table 2 lists the values of 1/n, K_f, and R^2, which were determined to be 0.928, 2.246 mg/g, and 0.902, respectively. Given the relatively good correlation coefficients obtained for both the Langmuir and Freundlich isotherm models, they were assumed to be suitable for explaining the sorption mechanism.

Table 2
Parameters of Freundlich Isotherm

Freundlich Isotherm	1/n	K_f (mg/g)	R^2
	0.928	2.246	0.902

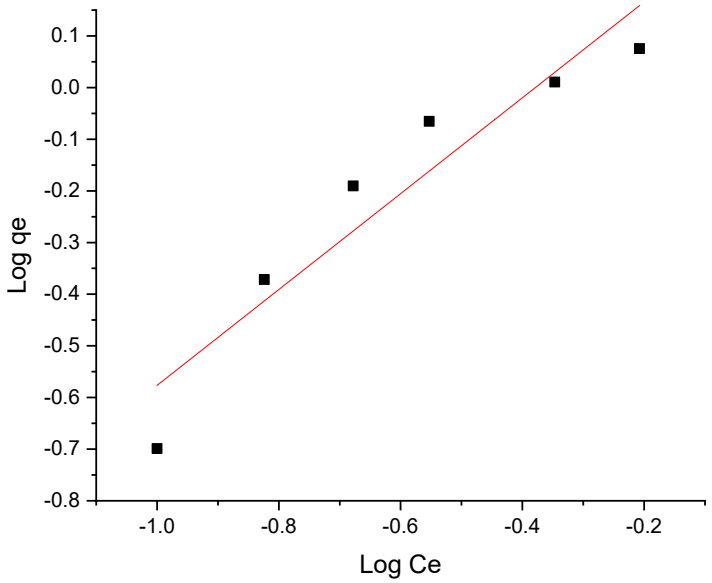

Fig. 8. Freundlich adsorption isotherm

4. Conclusions

In conclusion, MCC isolated from watermelon rind using acid hydrolysis, preceded by alkaline treatment and a bleaching process, was confirmed through FTIR analysis, which revealed the absence of absorbance bands at 1720, 1584, and 1242 cm^{-1} in the spectra of MCC. The SEM results demonstrated that the MCC exhibited a smooth surface, attributed to the removal of lignin and hemicellulose, and displayed a significant reduction in size following acid hydrolysis. The measured dimensions of MCC indicate a diameter of less than 74 µm and a length of less than 737 µm. Thermogravimetric analysis revealed that MCC underwent degradation earlier than watermelon rind, reaching its maximum degradation rate at 215°C, as evident in the DTG curve. Furthermore, the extracted MCC demonstrated its potential as an effective and economical adsorbent for removing dyes from industrial effluents. The effects of contact time and initial dye concentration on its adsorption capacity were studied, and the findings revealed that the most effective dye removal, reaching 86.32%, occurred when the methylene blue dye concentration was set at 1.5 mg/L. Moreover, the efficiency of dye removal experienced a swift rise, escalating from 67.34% to 80.73% with an increase in contact time from 20 to 60 minutes, after which the rate of increase notably decelerated. The adsorption data was validated using Langmuir and Freundlich isotherm models. The Langmuir constant value obtained was 0.8529, and the Freundlich constant value, representing the adsorption intensity, was 2.246 mg/g, indicating that dye adsorption by MCC is favourable.

The environmentally friendly nature of the MCC adsorbent makes it suitable for decolourisation purposes and offers an efficient and cost-effective solution for treating wastewater in the textile industry. Moreover, utilising MCC derived from watermelon rind presents a sustainable approach to address the disposal issue of watermelon rind waste in future landfills. By repurposing this waste material, the study reduces environmental burdens and promotes a circular economy. Moving forward, several recommendations are proposed for future research. Additional characterisations, such as BET analysis, Zeta potential measurement, and X-ray diffraction, can provide further insights into the adsorbent's surface properties and crystalline structure. Conducting further adsorption isotherm studies will also enhance the understanding of solute-adsorbent interactions and aid in determining optimal adsorption conditions. Moreover, exploring the application of MCC in treating different types of wastewater will help assess its potential and versatility. Overall, the findings underscore the promising prospects of MCC derived from watermelon rind in various applications, including wastewater treatment and waste management. Future research efforts can build upon these findings to further optimise the performance and expand the scope of MCC-based adsorbents as well as extend to NCC-based adsorbents. These include investigating the effects of adsorbent dose, pH, stirring rate, and different times to adsorb dye.

Acknowledgement
This research was not funded by any grant.

References

[1] Jenny Gustavsson, Christel Cederberg, Ulf Sonesson, Robert Otterdijk, and Alexandre Meybeck. "Global Food Losses and Food Waste- Extent, Causes and Prevention." (2011).

[2] Mason-D'Croz, Daniel, Jessica R. Bogard, Timothy B. Sulser, Nicola Cenacchi, Shahnila Dunston, Mario Herrero, and Keith Wiebe. "Gaps between fruit and vegetable production, demand, and recommended consumption at global and national levels: an integrated modelling study." *The Lancet Planetary Health* 3, no. 7 (2019): e318-e329. https://doi.org/10.1016/S2542-5196(19)30095-6

[3] Bharathi, K. S., and S. T. Ramesh. "Removal of dyes using agricultural waste as low-cost adsorbents: a review." *Applied water science* 3 (2013): 773-790. https://doi.org/10.1007/s13201-013-0117-y

[4] Achyuta Kumar Biswal, Laxmipriya Panda, Sourav Chakraborty, Subrat Kumar Pradhan, Manas Ranjan Dash, and Pramila Kumari Misra. "Production of a nascent cellulosic material from vegetable waste: Synthesis, characterization, functional properties, and its potency for a cationic dye removal." *International Journal of Biological Macromolecules* 242 (2023): 124959. https://doi.org/10.1016/j.ijbiomac.2023.124959

[5] Rasim Batmaz, Nishil Mohammed, Masuduz Zaman, Gagan Minhas, Richard M. Berry, and Kam C. Tam. "Cellulose nanocrystals as promising adsorbents for the removal of cationic dyes." *Cellulose* 21, no. 3 (2014): 1655-1665. https://doi.org/10.1007/s10570-014-0168-8

[6] Piaskowski, Krzysztof, Renata Świderska-Dąbrowska, and Paweł K. Zarzycki. "Dye removal from water and wastewater using various physical, chemical, and biological processes." *Journal of AOAC International* 101, no. 5 (2018): 1371-1384. https://doi.org/10.5740/jaoacint.18-0051

[7] Solayman, H. M., Md Arif Hossen, Azrina Abd Aziz, Noor Yahida Yahya, Kah Hon Leong, Lan Ching Sim, Minhaj Uddin Monir, and Kyung-Duk Zoh. "Performance evaluation of dye wastewater treatment technologies: A review." *Journal of Environmental Chemical Engineering* 11, no. 3 (2023): 109610. https://doi.org/10.1016/j.jece.2023.109610

[8] Nishil Mohammed. "Cellulose nanocrystals incorporated nanocomposites for water treatment applications." *UWSpace* (2017).

[9] Ruhma Rashid, Iqrash Shafiq, Parveen Akhter, Muhammad Javid Iqbal, and Murid Hussain. "A state-of-the-art review on wastewater treatment techniques: the effectiveness of adsorption method." *Environmental Science and Pollution Research* 28, no. 8 (2021): 9050-9066. https://doi.org/10.1007/s11356-021-12395-x.

[10] Princess C. Ani, Paul U. Nzereogu, Ada C. Agbogu, Fabian I. Ezema, and Assumpta C. Nwanya. "Cellulose from waste materials for electrochemical energy storage applications: A review." *Applied Surface Science Advances* 11 (2022): 100298. https://doi.org/10.1016/j.apsadv.2022.100298

[11] Velmurugan, Balasubramanian, Madhuri Narra, Darshan M. Rudakiya, and Datta Madamwar. "Sweet sorghum: a potential resource for bioenergy production." In *Refining biomass residues for sustainable energy and bioproducts*, pp. 215-242. Academic Press, 2020. https://doi.org/10.1016/B978-0-12-818996-2.00010-7.

[12] Manzato, L., L. C. A. Rabelo, S. M. De Souza, C. G. Da Silva, E. A. Sanches, D. Rabelo, L. A. M. Mariuba, and J. Simonsen. "New approach for extraction of cellulose from tucumã's endocarp and its structural characterization." *Journal of Molecular Structure* 1143 (2017): 229-234. https://doi.org/10.1016/j.molstruc.2017.04.088

[13] Ilham, Zul. "Biomass classification and characterization for conversion to biofuels." In *Value-chain of biofuels*, pp. 69-87. Elsevier, 2022. https://doi.org/10.1016/B978-0-12-824388-6.00014-2

[14] R. C. R. Nunes, *13 - Rubber nanocomposites with nanocellulose*, in *Progress in Rubber Nanocomposites*, S. ThomasH.J. Maria, Editors. 2017, Woodhead Publishing. p. 463-494. https://doi.org/10.1016/B978-0-08-100409-8.00013-9

[15] Kovalenko, Valeri I. "Crystalline cellulose: structure and hydrogen bonds." *Russian Chemical Reviews* 79, no. 3 (2010): 231. https://doi.org/10.1070/RC2010v079n03ABEH004065

[16] Wahlström, Niklas, Ulrica Edlund, Henrik Pavia, Gunilla Toth, Aleksander Jaworski, Andrew J. Pell, Ferdinand X. Choong, Hamid Shirani, K. Peter R. Nilsson, and Agneta Richter-Dahlfors. "Cellulose from the green macroalgae Ulva lactuca: isolation, characterization, optotracing, and production of cellulose nanofibrils." *Cellulose* 27 (2020): 3707-3725. https://doi.org/10.1007/s10570-020-03029-5

[17] Qiqi Wu, Jun Xu, Zhenhua Wu, Shiyun Zhu, Yi Gao, and Congcan Shi. "The effect of surface modification on chemical and crystalline structure of the cellulose III nanocrystals." *Carbohydrate Polymers* 235 (2020): 115962 . https://doi.org/10.1016/j.carbpol.2020.115962

[18] FFahma, F., I. Febiyanti, N. Lisdayana, I. W. Arnata, and D. Sartika. "Nanocellulose as a new sustainable material for various applications: A review." *Archives of Materials Science and Engineering* 109, no. 2 (2021): 49-64. https://doi.org/10.5604/01.3001.0015.2624

[19] Ahmad, Usama, and Juber Akhtar, eds. *Pharmaceutical Formulation Design: Recent Practices*. BoD–Books on Demand, 2020. https://doi.org/10.5772/intechopen.78460

[20] Zaharaddeen N. Garba, Ibrahim Lawan, Weiming Zhou, Mingxi Zhang, Liwei Wang, and Zhanhui Yuan. "Microcrystalline cellulose (MCC) based materials as emerging adsorbents for the removal of dyes and heavy metals – A review." *Science of The Total Environment* 717 (2020): 135070. https://doi.org/10.1016/j.scitotenv.2019.135070.

[21] Abida Kausar, Sadia Tul Zohra, Sana Ijaz, Munawar Iqbal, Jibran Iqbal, Ismat Bibi, Shazia Nouren, Noureddine El Messaoudi, and Arif Nazir. "Cellulose-based materials and their adsorptive removal efficiency for dyes: A review." *International Journal of Biological Macromolecules* 224 (2023): 1337-1355. https://doi.org/10.1016/j.ijbiomac.2022.10.220.

[22] Baoliang Peng, Zhaoling Yao, Xiaocong Wang, Mitchel Crombeen, Dalton G. Sweeney, and Kam Chiu Tam. "Cellulose-based materials in wastewater treatment of petroleum industry." *Green Energy & Environment* 5, no. 1 (2020): 37-49. https://doi.org/10.1016/j.gee.2019.09.003

[23] Trung Thanh Nguyen, Bao Tran Nguyen Thi, Phuoc Toan Phan, Tri Thich Le, Quynh Anh Nguyen Thi, Long Giang Bach, Thai Anh Nguyen, and Nhat Huy Nguyen. "Synthesis of microcrystalline cellulose from banana pseudo-stem for adsorption of organics from aqueous solution." *Engineering and Applied Science Research* 48, no. 4 (2021): 368-378.

[24] Hubbe, Martin A., and Orlando J. Rojas. "Colloidal stability and aggregation of lignocellulosic materials in aqueous suspension: A review." *BioResources* 3, no. 4 (2008): 1419-1491.

[25] Caryn Hui Chuin Tan, Sumiyyah Sabar, and M. Hazwan Hussin. "Development of immobilized microcrystalline cellulose as an effective adsorbent for methylene blue dye removal." *South African Journal of Chemical Engineering* 26 (2018): 11-24. https://doi.org/10.1016/j.sajce.2018.08.001

[26] M. Hazwan Hussin, Nurul Aqilah Pohan, Zaharaddeen N. Garba, M. Jain Kassim, Afidah Abdul Rahim, Nicolas Brosse, Mehdi Yemloul, M. R. Nurul Fazita, and M. K. Mohamad Haafiz. "Physicochemical of microcrystalline cellulose from oil palm fronds as potential methylene blue adsorbents." *International Journal of Biological Macromolecules* 92 (2016): 11-19. https://doi.org/10.1016/j.ijbiomac.2016.06.094

[27] Hongjuan Bai, Junhang Chen, Xiangyu Zhou, and Chengzhi Hu. "Single and binary adsorption of dyes from aqueous solutions using functionalized microcrystalline cellulose from cotton fiber." *Korean Journal of Chemical Engineering* 37, no. 11 (2020): 1926-1932. https://doi.org/10.1007/s11814-020-0621-3

[28] Sundarraj, Antony Allwyn, and Thottiam Vasudevan Ranganathan. "Comprehensive review on cellulose and microcrystalline cellulose from agro-industrial wastes." *Drug Invention Today* 10, no. 1 (2018): 2783-2788.

[29] Sohni, Saima, Shehla Begum, Rokiah Hashim, Sher Bahadar Khan, Faryal Mazhar, Fatima Syed, and Shahid Ali Khan. "Physicochemical characterization of microcrystalline cellulose derived from underutilized orange peel waste as a

sustainable resource under biorefinery concept." *Bioresource Technology Reports* 25 (2024): 101731. https://doi.org/10.1016/j.biteb.2023.101731

[30] Kari Vanhatalo, Natalia Maximova, Anna Maija Perander, Leena Sisko Johansson, Eero Haimi, and Olli Dahl. "Comparison of conventional and lignin-rich microcrystalline cellulose." *BioResources* 11, no. 2 (2016): 4037-4054. https://doi.org/10.15376/biores.11.2.4037-4054

[31] Zuliahani Ahmad, Nurul Nadhirah Roziaizan, Rozyanty Rahman, Ahmad Faiza Mohamad, and Wan Izhan Nawawi Wan Ismail. "Isolation and Characterization of Microcrystalline Cellulose (MCC) from Rice Husk (RH)." *MATEC Web of Conferences* 47 (2016): 05013. https://doi.org/10.1051/matecconf/20164705013

[32] Romario Abdullah, Dinia Astira, Utari Zulfiani, Alvin Rahmad Widyanto, Alvin Romadhoni Putra Hidayat, Dety Oktavia Sulistiono, Zeni Rahmawati, Triyanda Gunawan, Yuly Kusumawati, Mohd Hafiz Dzarfan Othman, and Hamzah Fansuri. "Fabrication of composite membrane with microcrystalline cellulose from lignocellulosic biomass as filler on cellulose acetate based membrane for water containing methylene blue treatment." *Bioresource Technology Reports* 25 (2024): 101728. https://doi.org/10.1016/j.biteb.2023.101728

[33] Banhisikha Debnath, Dibyajyoti Haldar, and Mihir Kumar Purkait. "A critical review on the techniques used for the synthesis and applications of crystalline cellulose derived from agricultural wastes and forest residues." *Carbohydrate Polymers* 273 (2021): 118537. https://doi.org/10.1016/j.carbpol.2021.118537

[34] Guillaume Chomicki, Hanno Schaefer, and Susanne S. Renner. "Origin and domestication of Cucurbitaceae crops: insights from phylogenies, genomics and archaeology." *New Phytologist* 226, no. 5 (2020): 1240-1255. https://doi.org/10.1111/nph.16015

[35] Sanwiriya, P., and N. Suleiman. "The effects of drying method and temperature on the nutritional quality of watermelon rinds." *International Food Research Journal* 26, no. 3 (2019): 953-958.

[36] Jun Seok Kim, Y. Y. Lee, and Tae Hyun Kim. "A review on alkaline pretreatment technology for bioconversion of lignocellulosic biomass." *Bioresource Technology* 199 (2016): 42-48. https://doi.org/10.1016/j.biortech.2015.08.085

[37] Christian J. Wijaya, Stephanie N. Saputra, Felycia E. Soetaredjo, Jindrayani N. Putro, Chun X. Lin, Alfin Kurniawan, Yi-Hsu Ju, and Suryadi Ismadji. "Cellulose nanocrystals from passion fruit peels waste as antibiotic drug carrier." *Carbohydrate Polymers* 175 (2017): 370-376. https://doi.org/10.1016/j.carbpol.2017.08.004

[38] Zahid Hanif, Hyeonyeol Jeon, Thang Hong Tran, Jonggeon Jegal, Seul- A. Park, Seon-Mi Kim, Jeyoung Park, Sung Yeon Hwang, and Dongyeop X. Oh. "Butanol-mediated oven-drying of nanocellulose with enhanced dehydration rate and aqueous re-dispersion." *Journal of Polymer Research* 25, no. 3 (2017): 191. https://doi.org/10.1007/s10965-017-1343-z

[39] Buong Woei Chieng, Syn Huey Lee, Nor Azowa Ibrahim, Yoon Yee Then, and Yuet Ying Loo. "Isolation and Characterization of Cellulose Nanocrystals from Oil Palm Mesocarp Fiber." *Polymers* 9, no. 8 (2017): 355. https://doi.org/10.3390/polym9080355

[40] Ibrahim, A., L. Yusof, N. S. Beddu, N. Galasin, P. Y. Lee, R. N. S. Lee, and A. Y. Zahrim. "Adsorption study of Ammonia Nitrogen by watermelon rind." In *IOP Conference Series: Earth and Environmental Science*, vol. 36, no. 1, p. 012020. IOP Publishing, 2016. https://doi.org/10.1088/1755-1315/36/1/012020

[41] Hengxiang Li, Kang Zhang, Xiaohua Zhang, Qing Cao, and Li'e Jin. "Contributions of ultrasonic wave, metal ions, and oxidation on the depolymerization of cellulose and its kinetics." *Renewable Energy* 126 (2018): 699-707. https://doi.org/10.1016/j.renene.2018.03.079

[42] Shamala Gowri Krishnan, Fei-ling Pua, and Fan Zhang. "Oil palm empty fruit bunch derived microcrystalline cellulose supported magnetic acid catalyst for esterification reaction: An optimization study." *Energy Conversion and Management: X* 13 (2022): 100159. https://doi.org/10.1016/j.ecmx.2021.100159

[43] Abeer M. Adel, Zeinab H. Abd El–Wahab, Atef A. Ibrahim, and Mona T. Al–Shemy. "Characterization of microcrystalline cellulose prepared from lignocellulosic materials. Part I. Acid catalyzed hydrolysis." *Bioresource Technology* 101, no. 12 (2010): 4446-4455. https://doi.org/10.1016/j.biortech.2010.01.047

[44] Haiwei Ren, Jiali Shen, Jiawen Pei, Zhiye Wang, Zhangpu Peng, Shanfei Fu, and Yi Zheng. "Characteristic microcrystalline cellulose extracted by combined acid and enzyme hydrolysis of sweet sorghum." *Cellulose* 26, no. 15 (2019): 8367-8381. https://doi.org/10.1007/s10570-019-02712-6

[45] Moufida Beroual, Lokmane Boumaza, Oussama Mehelli, Djalal Trache, Ahmed Fouzi Tarchoun, and Kamel Khimeche. "Physicochemical Properties and Thermal Stability of Microcrystalline Cellulose Isolated from Esparto Grass Using Different Delignification Approaches." *Journal of Polymers and the Environment* 29, no. 1 (2021): 130-142. https://doi.org/10.1007/s10924-020-01858-w

[46] Fouad, H., Lau Kia Kian, Mohammad Jawaid, Majed D. Alotaibi, Othman Y. Alothman, and Mohamed Hashem. "Characterization of microcrystalline cellulose isolated from conocarpus fiber." *Polymers* 12, no. 12 (2020): 2926. https://doi.org/10.3390/polym12122926

[47] Ahmed Fouzi Tarchoun, Djalal Trache, and Thomas M. Klapötke. "Microcrystalline cellulose from Posidonia oceanica brown algae: Extraction and characterization." *International Journal of Biological Macromolecules* 138 (2019): 837-845. https://doi.org/10.1016/j.ijbiomac.2019.07.176

[48] Nazir, Farzana, and Mudassir Iqbal. "Synthesis, characterization and cytotoxicity studies of aminated microcrystalline cellulose derivatives against melanoma and breast cancer cell lines." *Polymers* 12, no. 11 (2020): 2634. https://doi.org/10.3390/polym12112634

[49] Junidah Lamaming, Rokiah Hashim, Othman Sulaiman, Cheu Peng Leh, Tomoko Sugimoto, and Noor Afeefah Nordin. "Cellulose nanocrystals isolated from oil palm trunk." *Carbohydrate Polymers* 127 (2015): 202-208. https://doi.org/10.1016/j.carbpol.2015.03.043

[50] Christopher L. Waters, Rajiv R. Janupala, Richard G. Mallinson, and Lance L. Lobban. "Staged thermal fractionation for segregation of lignin and cellulose pyrolysis products: An experimental study of residence time and temperature effects." *Journal of Analytical and Applied Pyrolysis* 126 (2017): 380-389. https://doi.org/10.1016/j.jaap.2017.05.008

[51] Gamal Abdalla Suliman Haron, Hamayoun Mahmood, Hilmi Bin Noh, Masahiro Goto, and Muhammad Moniruzzaman. "Cellulose nanocrystals preparation from microcrystalline cellulose using ionic liquid-DMSO binary mixture as a processing medium." *Journal of Molecular Liquids* 346 (2022): 118208. https://doi.org/10.1016/j.molliq.2021.118208

[52] Aline Merlini, Carlos Claumann, André Wust Zibetti, André Coirolo, Tailin Rieg, and Ricardo A. F. Machado. "Kinetic Study of the Thermal Decomposition of Cellulose Nanocrystals with Different Crystal Structures and Morphologies." *Industrial & Engineering Chemistry Research* 59, no. 30 (2020): 13428-13439. https://doi.org/10.1021/acs.iecr.0c01444

[53] Nasrullah Razali, Md Sohrab Hossain, Owolabi Abdulwahab Taiwo, Mazlan Ibrahim, Nur Wahidah Mohd Nadzri, Nadilah Razak, Nurul Fazita Mohammad Rawi, Marliana Mohd Mahadar, and Mohamad Haafiz Mohamad Kassim. "Influence of acid hydrolysis reaction time on the isolation of cellulose nanowhiskers from oil palm empty fruit bunch microcrystalline cellulose." *BioResources* 12, no. 3 (2017): 6773-6788. https://doi.org/10.15376/biores.12.3.6773-6788

[54] Osman Gulnaz, Aysenur Kaya, Fatih Matyar, and Burhan Arikan. "Sorption of basic dyes from aqueous solution by activated sludge." *Journal of Hazardous Materials* 108, no. 3 (2004): 183-188. https://doi.org/10.1016/j.jhazmat.2004.02.012

[55] Ahmad Reza Yari, Gharib Majidi, Mehdi Tanhaye Reshvanloo, Mohsen ansari, Shahram Nazari, Meysam Emami Kale Sar, Mohammad Khazaei, and Maryam Sadat Tabatabai-Majd. "Using Eggshell in Acid Orange 2 Dye Removal from Aqueous Solution." *Iranian Journal Of Health Sciences* 3, no. 2 (2015): 38-45. http://dx.doi.org/10.7508/ijhs.2015.02.006

[56] Bishnupriya Nayak, Amruta Samant, Rajkishore Patel, and Pramila K. Misra. "Comprehensive Understanding of the Kinetics and Mechanism of Fluoride Removal over a Potent Nanocrystalline Hydroxyapatite Surface." *ACS Omega* 2, no. 11 (2017): 8118-8128. https://doi.org/10.1021/acsomega.7b00370

[57] Tawfik A. Saleh, *Chapter 4 - Isotherm models of adsorption processes on adsorbents and nanoadsorbents*, in *Interface Science and Technology*, T.A. Saleh, Editor. 2022, Elsevier. p. 99-126. https://doi.org/10.1016/B978-0-12-849876-7.00009-9

[58] Laxmipriya Panda, Swagat S. Rath, Danda Srinivas Rao, Binod B. Nayak, Bisweswar Das, and Pramila K. Misra. "Thorough understanding of the kinetics and mechanism of heavy metal adsorption onto a pyrophyllite mine waste based geopolymer." *Journal of Molecular Liquids* 263 (2018): 428-441. https://doi.org/10.1016/j.molliq.2018.05.016

[59] Sun, Wenguang, and H. Magdi Selim. "Fate and transport of molybdenum in soils: Kinetic modeling." *Advances in Agronomy* 164 (2020): 51-92. https://doi.org/10.1016/bs.agron.2020.06.002

[60] Proctor, A. U. O. A., and J. F. Toro-Vazquez. "The Freundlich isotherm in studying adsorption in oil processing." *Journal of the American Oil Chemists' Society* 73 (1996): 1627-1633. https://doi.org/10.1016/B978-1-893997-91-2.50016-X